Original Article

Loading MicroRNA-376c in Extracellular Vesicles Inhibits Properties of Non-Small Cell Lung Cancer Cells by Targeting YTHDF1

Jianying Zhou, MM[1], Dan Xiao, MM[1], Tingting Qiu, MM[1], Jun Li, MM[1], and Zhentian Liu, MM[1]

Abstract

Objective: Extracellular vesicles (Evs) secreted from cells have been revealed to mediate signal transduction between cells. Nevertheless, the mechanisms through which molecules transported by EVs function remain to be elucidated. In the present study, the functional relevance of endothelial cells (ECs)-secreted Evs carrying microRNA-376c (miR-376c) in the biological activities of non-small cell lung cancer (NSCLC) cells was investigated, including the related mechanisms. **Methods:** Two cell lines with the highest YTH N6-methyladenosine (m6A) RNA binding protein 1 (YTHDF1) expression were selected for subsequent experiments. Cellular proliferation, migration, invasion and apoptosis were measured by EdU, wound healing, Transwell assays and flow cytometry, respectively. The binding relationship between miR-376c and YTHDF1 was analyzed by dual-luciferase reporter assays. The miR-376c, YTHDF1 and β-catenin expression was evaluated by qPCR assays and western blot assays. **Results:** The expression patterns of YTHDF1 were higher in NSCLC cells, whereas miR-376c was reduced versus the normal bronchial epithelial cells. Silencing of YTHDF1 repressed NSCLC cell proliferation, invasion and migration abilities, whereas enhanced apoptosis. miR-376c negatively modulated YTHDF1 expression. Under co-culture conditions, ECs transmitted miR-376c into NSCLC cells through Evs, and inhibited the intracellular YTHDF1 expression and the Wnt/β-catenin pathway activation. Rescue experiments revealed that YTHDF1 overexpression reversed the inhibitory role of miR-376c released by EC-Evs in NSCLC cells. **Conclusion:** EC-delivered Evs inhibit YTHDF1 expression and the Wnt/β-catenin pathway induction via miR-376c overexpression, thus inhibiting the malignant phenotypes of NSCLC cells.

Keywords

microRNA-376c, YTHDF1, non-small cell lung cancer, extracellular vesicles, the Wnt/β-catenin pathway

Introduction

Lung cancer had the highest incidence and mortality rates among all cancer types in 2018 globally, with the death rate close to 1 in 5 (18.4%) and the highest incidence rate among male observed in China.[1] Non-small-cell lung cancer (NSCLC) contributes to approximately 80-85% of all lung cancer cases, and improvements in surgery, chemotherapy and radiotherapy have not contributed to significant progress in terms of prognosis, thus innovative biomarkers that could improve diagnosis and prognostic stratification are urgently required.[2] Cell-cell contact or the transmission of secreted molecules in a direct manner has been recognized as the 2 main means for intercellular communication, in addition to physical force, geometric constraints and mechanobiological factors, while a third mechanism involving the intercellular transfer of extracellular vesicles (Evs) has recently emerged.[3] Moreover, exosomes, ranging from 30 to 150 nm in size, transport different types of biomolecules, such as proteins, messenger RNAs (mRNAs)

[1] Department of Thoracic Oncology, Jiangxi Cancer Hospital, Nanchang, Jiangxi, People's Republic of China

Corresponding Author:
Zhentian Liu, Department of Thoracic Oncology, Jiangxi Cancer Hospital, No. 519, East Beijing Road, Qingshanhu District, Nanchang 330029, Jiangxi, People's Republic of China.
Email: liuzhentian12091@163.com

as well as microRNAs (miRNAs or miRs) between cells.[4] Exosomes released from umbilical vein endothelial cells (ECs) facilitate the expansion of neural stem cells.[5] However, the effects of EC-derived Evs on the biological activities of NSCLC cells have not yet been determined.

The importance of miRNAs in cancers has become increasingly clear when bearing in mind that almost half of all miRNAs are located at fragile regions or cancer-related genomic sites that are commonly cancelled or augmented in tumorigenesis.[6] For instance, the enforced expression of miR-376c has been shown to attenuate the proliferation and invasion of NSCLC cells and the induction of the Wnt pathway, whereas a decrease in miR-376c has been shown to reverse these effects.[7] Furthermore, miR-376c-3p has been evidenced to be profoundly downregulated in both maternal and umbilical cord serum-released exosomes.[8] Mechanistically, YTH N6-methyladenosine (m6A) RNA binding protein 1 (YTHDF1) was confirmed as a possible target for miR-376c in NSCLC cells in the present study by a dual-luciferase reporter gene assay. YTHDF1 exhibits a high expression in hepatocellular carcinoma, which is positively associated with the pathological stage of the patients, indicating its role as a possible therapeutic and prognostic target for cancers.[9] Moreover, YTHDF1 has been shown to be upregulated in colorectal cancer and to function as an oncogene, while the knockdown of YTHDF1 has been displayed to significantly disrupt the Wnt/β-catenin pathway in colorectal cancer cells.[10] Therefore, the effects of miR-376c secreted by EC-derived Evs on NSCLC cell activities including proliferation, migration, invasion and apoptosis were investigated in the present study. In addition, the underlying mechanisms were determined. The roles of miR-376c in the disruption of the Wnt/β-catenin pathway *in vitro* in a YTHDF1-dependent manner were also further examined.

Material and Methods

Gene Expression Omnibus (GEO) Analysis

The expression of YTHDF1 and miR-376c in lung cancer was obtained from the GEO (www.ncbi.nlm.nih.gov/geo/) online database. Expression of YTHDF1 in NSCLC tissues and normal lung tissues was obtained from dataset GSE63459 based on the GPL6883 Illumina HumanRef-8 v3.0 expression beadchip platform. The expression of miR-376c in NSCLC tissues and normal lung tissues was obtained from the dataset GSE53882 based on the GPL18130 State Key Laboratory Human microRNA array 1888 platform. SPSS21.0 was used to statistically analyze the datasets to examine the differential expression of YTHDF1 and miR-376c in NSCLC tissues and normal lung tissues.

Cell Lines Used and Cell Culture

Human normal bronchial epithelial cells 16HBE in addition to NSCLC cells A549, NCI-H358, NCI-H1299 and NCI-1650 (Shanghai Zhong Qiao Xin Zhou Biotechnology Co., Ltd., Shanghai, China) were cultivated with Roswell Park Memorial Institute-1640 medium (Gibco) containing 10% fetal bovine serum (FBS, Gibco) and penicillin/streptomycin (100 mg/mL). Human pulmonary microvascular ECs (Shanghai Zhong Qiao Xin Zhou Biotechnology) were cultivated in EC-specific totipotent medium (No.1001, Shanghai Zhong Qiao Xin Zhou Biotechnology) with 500 mL basic medium, 25 mL FBS, 5 mL endothelial cell growth factor and 5 mL penicillin/streptomycin solution at 37°C with 5% CO_2. NSCLC cells and ECs up to 85% confluence were used for subculture based on the observations of cell condition.

Cell Transfection

ECs were transfected with miR-376c mimic or mimic negative control (NC). While NCI-H1299 and NCI-1650 cells were treated with sh-YTHDF1 alone or pcDNA-YTHDF1 and then co-cultured with ECs after transfection.

Plasmids used for transfection (2.5 μg) were obtained from GenePharma Ltd. Company (Shanghai, China). Before transfection, cells were plated in 96-well plates for a period of 24 h. Once the cell density reached about 70-90%, we transfected cells following the protocols of Lipofectamine 2000 (11668-019, Invitrogen Inc., Carlsbad, CA, USA). At 48 h post-transfection, the transfection efficiency was checked by RT-qPCR, and subsequent experiments were performed.

Co-Culture System and GW4869 Treatment

ECs and NCI-H1299 or NCI-H1650 cells 48 h post-transfection were co-cultured in the Transwell plate. ECs were seeded in the apical chamber and NCI-H1299 or NCI-H1650 cells in the basolateral chamber with their respective culture media. After a total of 12 h of incubation, the NSCLC cells located in the basolateral chamber were collected for subsequent experiments.

To demonstrate that ECs delivered miR-376c via Evs, we treated ECs overexpressing miR-376c with 10 μM Evs inhibitor GW4869 (MedChemExpress, Monmouth Junction, NJ, USA) for 12 h and then co-cultured with NSCLC cells.

Immunofluorescence Staining

Cells cultured on the culture plate were covered with a layer of 2-3 mm 4% formaldehyde diluted with phosphate buffer saline (PBS) at room temperature for 15 min. After being sealed with the blocking buffer for 60 min, the cells were probed with the primary antibodies against YTHDF1 (#86463, Cell Signaling Technologies (CST), Beverly, MA, USA) and β-catenin (#8480, CST) at 4°C overnight. After diluting the fluorescent labeled secondary antibody (#4412, CST) with antibody dilution buffer, the cells were incubated at room temperature without light for 1-2 h. The cells were finally sealed with fluorescence quenching Prolong® Gold antifade reagent containing 4',6-diamidino-2-phenylindole (#8961, CST) and observed under a fluorescence microscopy (Leica Microsystems GmbH, Wetzlar, Germany) at 450 nm.

Dual-luciferase Reporter Gene Assay

The YTHDF1-3'untranslated region (3'UTR) containing the binding sites with miR-376c was inserted into the pGL3 plasmid (Promega, Madison, WI, USA). The YTHDF1-3'UTR-mutant (MUT) fragment of the binding site mutation was constructed by point mutation method using point mutation kits (Robustnique Corporation Ltd., Tianjin, China). "UAUUUGUACUUUUUCUAUGUA" was mutated to "UAUAUCUCAAUUAGAUACAA" on the YTHDF1-3'UTR and inserted into the pGL3 plasmids to construct the YTHDF1-MUT. The indicated plasmids and Renilla plasmid were introduced with miR-376c mimic or NC-mimic into HEK293 T cells (American Type Culture Collection, Manassas, VA, USA). Cells were lysed following 48 h of transfection under the instructions of a luciferase detection kit (K801-200, BioVision, Inc., Exton, PA, USA). Dual-luciferase reporter gene assays were carried out with the help of the Dual-Luciferase Reporter Assay System (Promega). Renilla activity served as the internal control.

5-Ethynyl-2'-Deoxyuridine (EdU) Staining

EdU kits (Thermo Fisher Scientific Inc., Waltham, MA, USA) were applied for proliferation assay. The cells were stained with EdU at room temperature for 2 h, treated for 30 min with 40 g/L paraformaldehyde and cultured for 8 min with glycine solution. After being rinsed with PBS/0.5% TritonX-100, the cells were treated successively for 30 min with Apollo® staining reaction solution and for 20 min with Hoechst 3334 staining solution at room temperature in darkness. The images were obtained under a fluorescence microscope under 3 field at 400 times. The proliferating cells (stained with EdU) and the total cells (stained with Hoechst 33342) were counted to calculate the cell proliferation rate.

Would Healing Assay

After 48 h, treated cells were plated in the 6-well plate at 5×10^5 cells/well. A sterile pipette was applied to scratch the central axis of the well when cells were covered with 90% microscopic view. After the removal of floating cells with PBS, the cells were further cultivated for 0.5 to 1 h with serum-free medium. The cell migration distances at the 0th h and 24th h were measured by Image-Pro Plus Analysis software (Media Cybernetics, Bethesda, MD, USA).

Transwell Assay

After 48 h of cell transfection, Matrigel (356234, BD Biosciences, San Jose, CA, USA) was liquefied overnight at 4°C, diluted at 1:3 with serum-free medium and cultured in the apical chamber (50 µL each well) for 30 min. The cell suspension was placed in the apical chamber at 1×10^5 cells/mL with serum-free medium. The chemoattractant in the basolateral chamber was culture medium plus 10% FBS. The plate was then incubated at 37°C for 24 h. Following the discarding of the non-invading cells by PBS, the remaining cells were fixed with

Table 1. Prime Sequences for Reverse Transcription-Quantitative Polymerase Chain Reaction.

Gene	Sequence (5'-3')
miR-376c	F: AACATAGAGGAAATTCCACGT
	R: CTCTACAGCTATATTGCCAGCCA
YTHDF1	F: ATACCTCACCACCTACGGACA
	R: GTGCTGATAGATGTTGTTCCCC
GAPDH	F: GGGAAACTGTGGCGTGAT
	R: GAGTGGGTGTCGCTGTTGA
U6	F: ATTGGAACGATACAGAGAAGATT
	R: GGAACGCTTCACGAATTTG

Note: miR-376c, microRNA-376; YTHDF1, YTH N6-methyladenosine (m6A) RNA binding protein 1; GAPDH, glyceraldehyde-3-phosphate dehydrogenase.

5% glutaraldehyde at 4°C, reacted for 30 min with 0.1% crystal violet and observed under a microscope.

Flow Cytometry for Cell Apoptosis

Annexin V-fluorescein isothiocyanate (FITC)/propidium iodide (PI) dual staining was applied for cell apoptosis. The cells were grown with 5% CO_2 at 37°C for 48 h. Following a centrifugation and resuspension in 200 µL binding buffer, the cells were treated with 10 µL Annexin V-FITC (ab14085, Abcam) and 5 µL PI for 15 min at ambient temperature void of light. Following adding 300 µL binding buffer, the cells were loaded onto a FACSVerse flow cytometer (BD Biosciences) at 488 nm. FlowJo software (Tree Star Inc., Ashland, OR, USA) was applied to quantify apoptosis rate.

Western Blot Analysis

After a 20-min centrifugation at 3000 r/min at 4°C, the cells were ice-bathed for 30 min with lysis buffer supplemented with proteinase inhibitor (1111111, Roche Diagnostics, Co., Ltd., Rotkreuz, Switzerland) and centrifuged at 12000 r/min for 10 min. Then, 50 µg protein was resolved by 10% sodium dodecyl sulfate-polyacrylamide gel electrophoresis and then trans-blotted to a polyvinylidene fluoride membrane which was blocked at room temperature with 5% skim milk powder for 1 h and probed overnight with the primary antibody at 4°C. Antibodies used were YTHDF1 (1:1000, ab99080, Abcam, Cambridge, UK), β-catenin (1:1000, ab2365, Abcam), glyceraldehyde-3-phosphate dehydrogenase (GAPDH, 1:2000, ab37168, Abcam) and horseradish peroxidase-labeled goat anti-rabbit antibody to IgG (1:100, HA1003, Shanghai Yanhui Biotechnology Co., Ltd., Shanghai, China). Blots were visualized with enhanced chemiluminescence reagent (ECL808-25, Biomiga, San Diego, CA, USA) and exposed to X-ray (Qcbio Science & Technologies Co., Ltd., Shanghai, China).

Reverse Transcription-Quantitative Polymerase Chain Reaction (RT-qPCR)

The total RNA was isolated from samples under the instructions of a miRNeasy Mini Kit (217004, Qiagen company, Hilden, Germany). All primers were synthesized by Takara Holdings Inc. (Kyoto, Japan) (Table 1). The RNA was then reversely
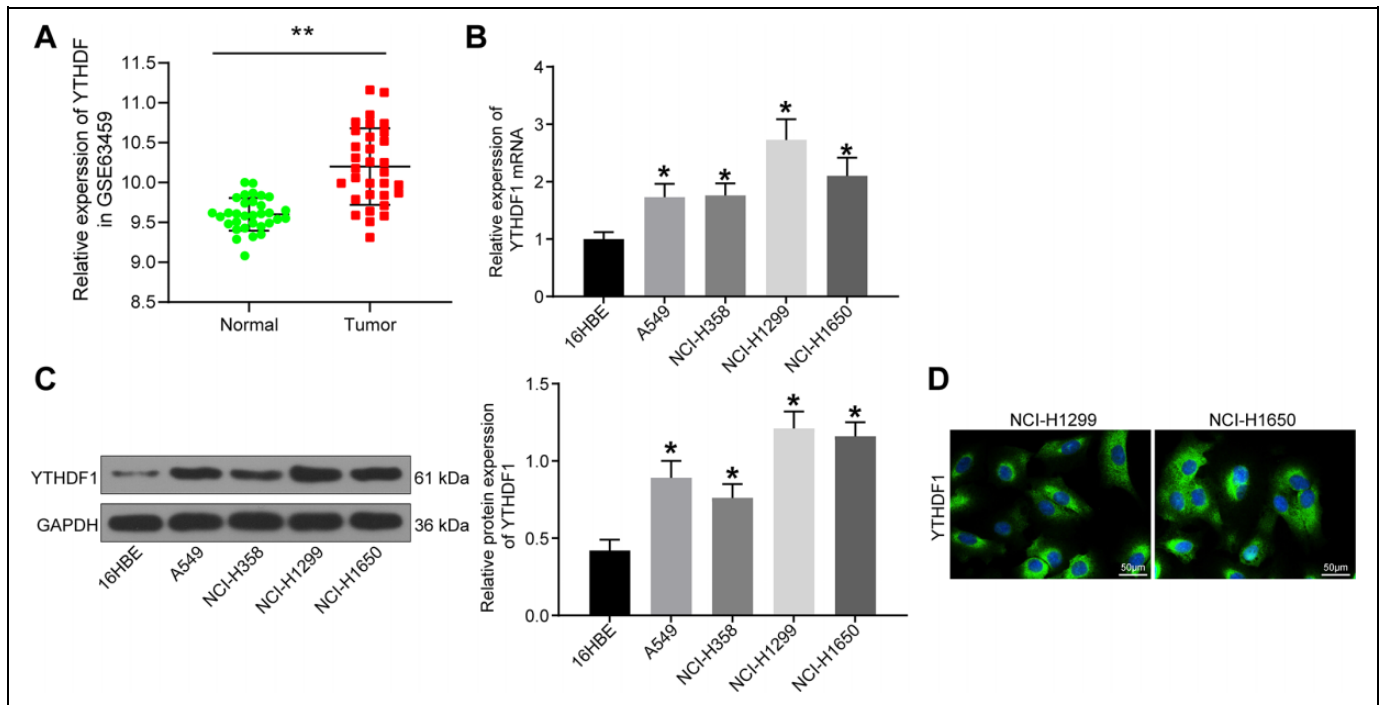
Figure 1. YTHDF1 is an oncogene in NSCLC cells. (A) GEO database query of YTHDF1 expression in normal lung and lung cancer tissues; (B) the mRNA expression of YTHDF1 in 16HBE and A549, NCI-H358, NCI-H1299 and NCI-1650 cells evaluated by RT-qPCR; (C) the protein expression of YTHDF1 in 16HBE and A549, NCI-H358, NCI-H1299 and NCI-1650 cells evaluated by western blot analysis; (D) location of YTHDF1 in NSCLC cells detected by immunofluorescence staining, where green fluorescence represents YTHDF1, blue is the nucleus stained by DAPI. $**p < 0.01$ *vs.* normal lung tissues; $*p < 0.05$ *vs.* 16HBE cells. Statistical data were measurement data, and described as mean $\pm$ standard deviation. The one-way analysis of variance with Tukey's post hoc test was used for comparison among multiple groups. The experiment was repeated 3 times independently.

transcribed into cDNA using the PrimeScript RT kit (RR036A, Takara). Next, the fluorescence quantitative PCR was conducted with reference to the SYBR® Premix ExTaq™ II kit (RR820A, TaKaRa) on an ABI 7500 quantitative PCR instrument (7500, ABI Company, Oyster Bay, N.Y., USA). All samples were normalized to U6 and GAPDH with the $2^{-\triangle\triangle CT}$ formula.

Statistics

Statistical computations were completed with the SPSS 21.0 (IBM SPSS Statistics, Chicago, IL, USA). Results were demonstrated as mean $\pm$ standard deviation. One-way or two-way analysis of variance followed by Tukey's post hoc test were applied for comparisons among multiple groups. p-value < 0.05 was considered to be significant statistically.

Results

YTHDF1 Expresses at a High Level in NSCLC Cells

With the aim to examine the mechanism of YTHDF1 in NSCLC cells, we queried the expression of YTHDF1 in NSCLC in the GEO dataset GSE63459 and found that its expression in tumor samples was generally higher than its expression in normal samples (Figure 1A). Afterward, 16HBE and A549, NCI-H358, NCI-H1299 and NCI-1650 cells were harvested to measure the

expression patterns of YTHDF1 using RT-qPCR and Western blot. As displayed in Figure 1B and C, the expression of YTHDF1 in A549, NCI-H358, NCI-H1299 and NCI-1650 cells was higher compared with 16HBE cells ($p < 0.05$), among which NCI-H1299 and NCI-1650 had the highest expression of YTHDF1, so these 2 cell lines were selected for the following experiments. The localization of YTHDF1 in both cells was detected by immunofluorescence staining, which revealed that it localized in the cytoplasm (Figure 1D).

YTHDF1 Silencing Suppresses NSCLC Cell Proliferation and Facilitates Apoptosis

YTHDF1 was then knocked-down in NCI-H1299 and NCI-1650 cells by sh-RNA, and the YTHDF1 silencing effect was confirmed by the means of RT-qPCR (Figure 2A). Moreover, we assessed the functional relevance of YTHDF1 to cell viability and apoptosis using EdU staining and flow cytometry (Figure 2B, C). As expected, cell proliferation was decreased significantly at 48 h and 72 h, while the apoptosis rate increased significantly after YTHDF1 silencing ($p < 0.05$).

YTHDF1 Silencing Represses NSCLC Cell Aggressiveness

We detected cell migration ability in NSCLC cells transfected with sh-NC and sh-YTHDF1 by wound healing assay and cell
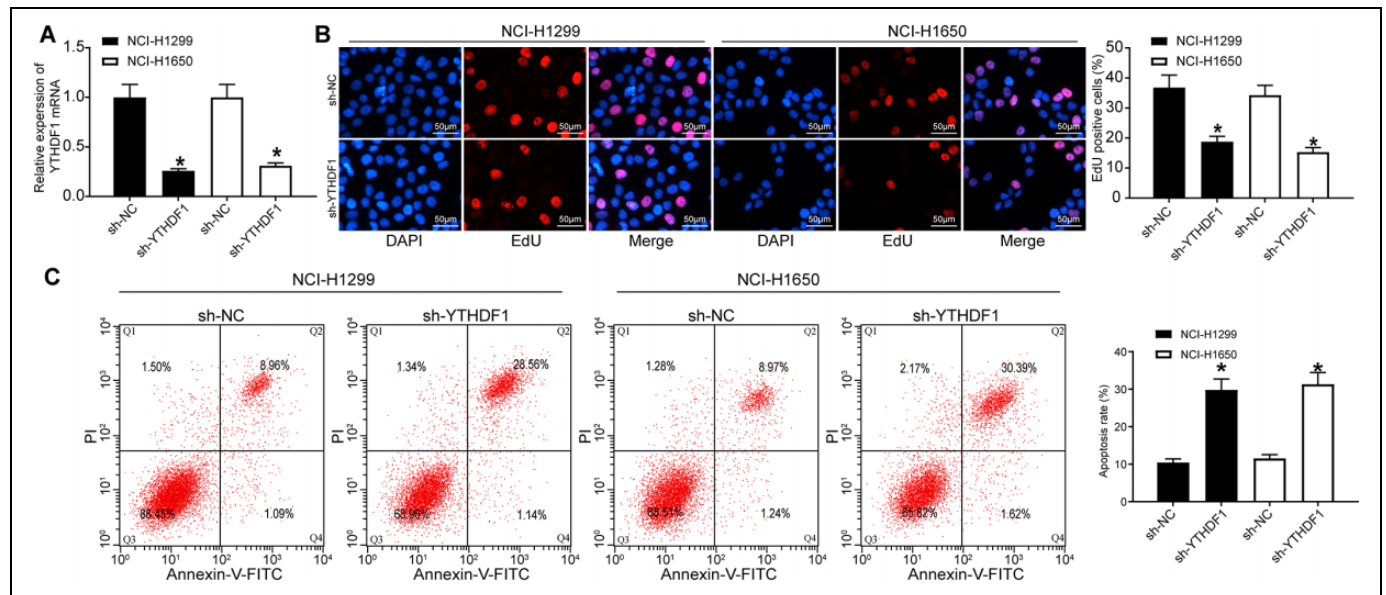
Figure 2. YTHDF1 depletion inhibits NSCLC cell viability, while promotes its apoptosis. (A) YTHDF1 mRNA expression after silencing YTHDF1 in NSCLC cells determined by RT-qPCR; (B) the cellular growth was analyzed by EdU assay in NSCLC cells (×200); (C) the apoptosis rate of cells was detected by flow cytometry. *$p < 0.05$ vs.* NSCLC cells transfected with sh-NC. Statistical data were measurement data, and described as mean $\pm$ standard deviation. The one-way analysis of variance with Tukey's post hoc test was used for comparison among multiple groups. The experiment was repeated 3 times independently.
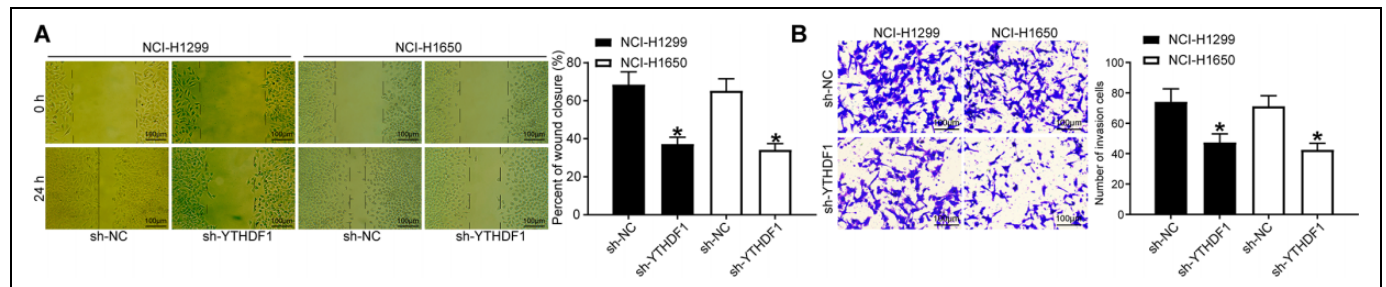

Figure 3. YTHDF1 silencing inhibits NSCLC cell migration and invasion. (A) The cell migration capacity was analyzed by wound healing assay (×100); (B) the cell invasion capacity was analyzed by Transwell assay (×100). *$p < 0.05$ vs.* NSCLC cells transfected with sh-NC. Statistical data were measurement data, and described as mean $\pm$ standard deviation. The one-way analysis of variance with Tukey's post hoc test was used for comparison among multiple groups. The experiment was repeated 3 times independently.

invasion ability by Transwell assay. The results showed that (Figure 3A, B): compared with sh-NC, the cell proliferation migration distance was significantly reduced after the sh-YTHDF1 transfection, and the number of invaded cells was also significantly decreased (both *$p < 0.05$*).

miR-376c Directly Targets YTHDF1 in NSCLC Cells

According to a previous report,[7] miR-376c was poorly expressed in NSCLC. We queried the GEO dataset GSE53882 for miR-376c expression in NSCLC tumor tissues and normal lung tissues and found that its expression was generally reduced in lung cancer tissues (Figure 4A). The miR-376c-binding sites in YTHDF1 3'UTR were predicted using an online website (Figure 4B, http://starbase.sysu.edu.cn/). Besides, we carried

out RT-qPCR to determine the miR-376c expression profile in normal bronchial epithelial cells 16HBE and NSCLC cells A549, NCI-H358, NCI-H1299 and NCI-1650. The results showed that (Figure 4C): compared with 16HBE cells, A549, NCI-H358, NCI-H1299 and NCI-1650 cells demonstrated reduced miR-376c expression. It was elucidated by the dual-luciferase reporter gene assays that miR-376c decreased the luciferase activities by targeting YTHDF1 3'UTR in 293 T cells. Nevertheless, the inhibitory effect was not showed in the cells when the binding sites were mutated (Figure 4D), suggesting that YTHDF1 mRNA is a new target of miR-376c.

EC-Evs Deliver miR-376c to NSCLC Cells

It has been reported that Evs of ECs could transfer tumor suppressors to tumor cells under co-culture conditions, thus
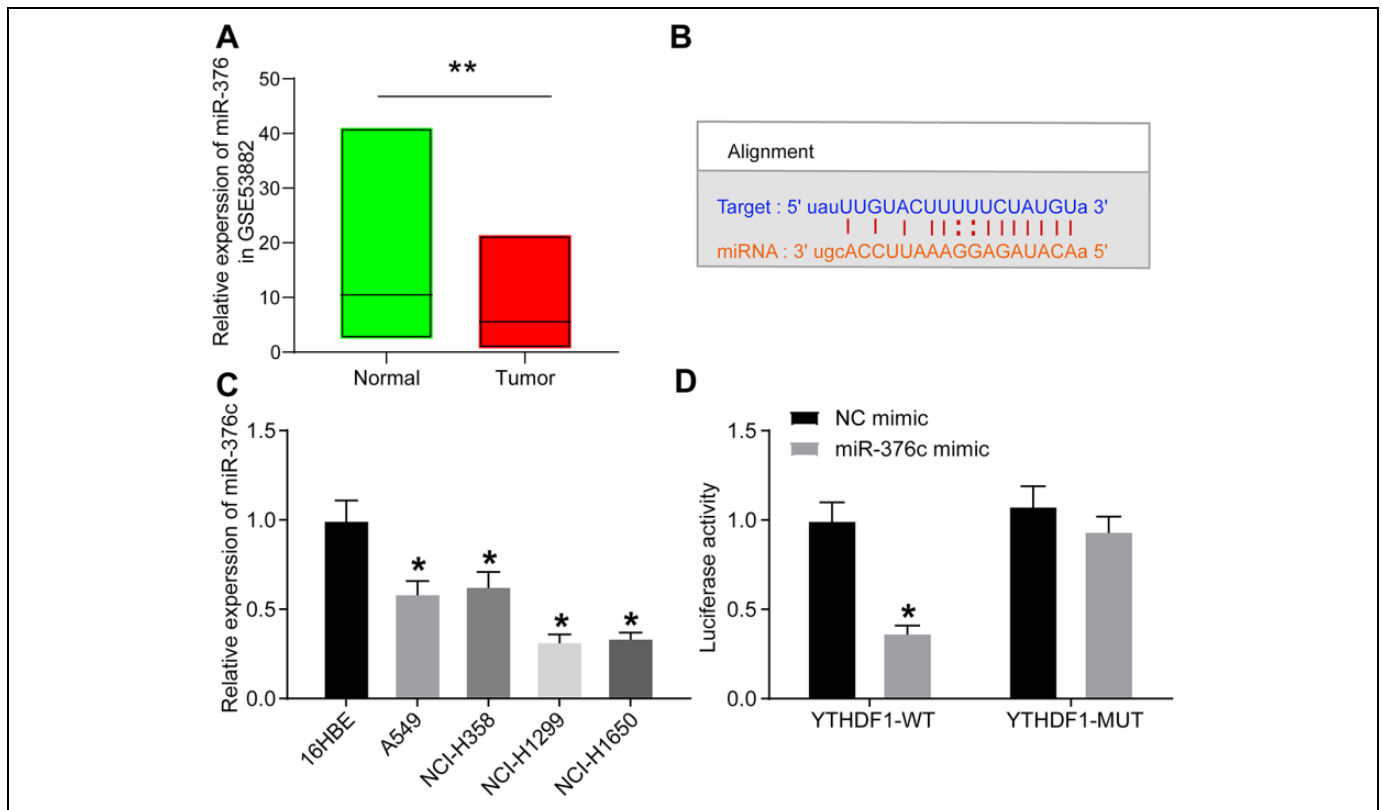
Figure 4. YTHDF1 could be targeted and inhibited by miR-376c. (A) Expression of miR-376c in NSCLC by querying miR-376c in the GEO dataset; (B) the sequences of miR-376c and its putative target sites in the 3'UTR of YTHDF1; (C) the expression of miR-376c in 16HBE, A549, NCI-H358, NCI-H1299 and NCI-1650 cells evaluated by RT-qPCR; (D) YTHDF1 3'UTR dual-luciferase reporter assay. **$p < 0.01$ *vs.* normal lung tissues; *$p < 0.05$ *vs.* 16HBE cells or NC mimic. Statistical data were measurement data, and described as mean $\pm$ standard deviation. The one-way or two-way analysis of variance with Tukey's post hoc test was used for comparison among multiple groups. The experiment was repeated 3 times independently.

inhibiting tumor cell activity and angiogenesis.[11] Therefore, it was assumed that ECs overexpressing miR-376c, under co-culture conditions, could deliver miR-376c to NSCLC cells through Evs, thereby inhibiting the expression of its target gene YTHDF1 and then inhibiting the biological properties of NSCLC cells. Firstly, we transfected miR-376c mimic into ECs. RT-qPCR evaluation of miR-376c expression showed that (Figure 5A): the expression of miR-376c was significantly increased in ECs overexpressing miR-376c compared to ECs harboring NC mimic ($p < 0.05$). ECs overexpressing miR-376c were then co-cultured with NSCLC cells in the Transwell plate. After 24 h, we evaluated miR-376c expression in NSCLC cells with the help of RT-qPCR. miR-376c expression was remarkably elevated in the NSCLC cells co-cultured with ECs harboring miR-376c mimic (Figure 5B; $p < 0.05$). To verify that miR-376c was delivered from ECs to NCI-H1299 and NCI-1650 cells via Evs, we added the Ev inhibitor GW4869 to the culture medium, and found that miR-376c expression was much lower following miR-376c mimic + GW4869 treatment than that after miR-376c mimic + DMSO (Figure 5C; $p < 0.05$). It can be concluded that under co-culture conditions, EC-Evs have the potency to deliver miR-376c to NCI-H1299 and NCI-1650 cells.

NSCLC Cell Activities Are Suppressed by miR-376c Released From EC-Evs

Under co-culture conditions, the proliferation, invasion and migration capacities of NCI-H1299 and NCI-1650 cells were assessed by EdU assay, wound healing assay and Transwell test, respectively, and the apoptosis was examined by flow cytometric analysis. It was displayed that the NSCLC cell proliferation was profoundly reduced at 48 and 72 h after miR-376c mimic treatment, the NSCLC cell migration and invasion were remarkably diminished, and the apoptosis was markedly enhanced (Figure 6A-D, all $p < 0.05$).

Release of miR-376c From EC-Evs Inhibits Activation of the Wnt/β-catenin Pathway in NSCLC Cells

The expression of YTHDF1 and Wnt/β-catenin pathway-associated protein β-catenin in NCI-H1299 and NCI-1650 cells co-cultured with ECs overexpressing miR-376c was subsequently measured by Western blot analysis. Figure 7A exhibits that YTHDF1 and β-catenin expression was significantly decreased in NCI-H1299 and NCI-1650 cells after miR-376c mimic introduction ($p < 0.05$). Immunofluorescence staining
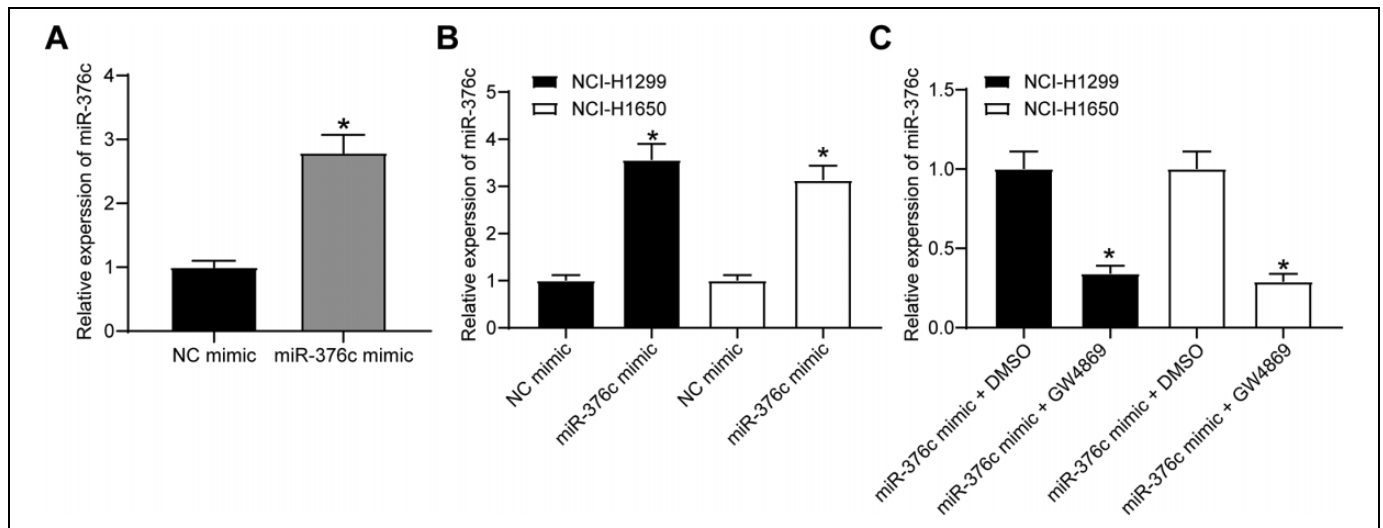
Figure 5. miR-376c is transferred by EC-Evs into NCL-H1299 cells. (A) Transfection efficiency of miR-376c mimic in ECs detected by RT-qPCR, *$p < 0.05$ *vs.* ECs transfected with NC mimic; (B) miR-376c expression in NSCLC cells co-cultured with ECs transfected with NC mimic or miR-376c mimic measured by RT-qPCR, *$p < 0.05$ *vs.* NSCLC cells co-cultured with ECs transfected with NC mimic; (C) miR-376c expression in NSCLC cells co-cultured with ECs treated with miR-376c mimic plus GW4869 or DMSO measured by RT-qPCR, *$p < 0.05$ *vs.* NSCLC cells co-cultured with ECs treated with miR-376c mimic + DMSO. Statistical data were measurement data, and described as mean $\pm$ standard deviation. The one-way analysis of variance with Tukey's post hoc test was used for comparison among multiple groups. The experiment was repeated 3 times independently.

revealed that β-catenin was distributed in the cytoplasm and nucleus of NSCLC cells (Figure 7B).

Overexpression of YTHDF1 Attenuates the Inhibitory Effect of miR-376c Released From EC-Evs on NSCLC Cell Growth

NSCLC were transfected pcDNA-YTHDF1 and then co-cultured with ECs. The expression of YTHDF1 and Wnt/β-catenin signaling pathway-related protein β-catenin in each group of cells was determined by western blot (Figure 8A, $p < 0.05$), which revealed that YTHDF1 overexpression could reverse the suppressive role of miR-376c mimic in β-catenin expression. The proliferation and apoptosis of cells in each group were measured by EdU and flow cytometry (Figure 8B, C). We found that inhibition of NSCLC growth induced by miR-376c mimic could be significantly reversed by YTHDF1 overexpression.

Overexpression of YTHDF1 Attenuates the Inhibitory Effect of miR-376c Released From EC-Evs on NSCLC Cell Migratory and Invasion

Wound healing and Transwell assays were performed to detect changes in cell migration and invasion capacities, and the results are shown in Figure 9A, B. The migration and invasion capacities of cells after overexpression of YTHDF1 was significantly inhibited (both $p < 0.05$).

Overall, under co-culture conditions, EC-Evs are capable of delivering miR-376c to NCI-H1299 and NCI-1650 cells, thereby inhibiting YTHDF1 expression and the activation of the Wnt/β-catenin pathway. As a result, the NSCLC cell

proliferation, migration and invasion are disrupted and apoptosis rate is accelerated.

Discussion

Considerable progress has been achieved in the diagnosis and therapeutic strategies for lung cancer recently; thus, the survival of patients with lung cancer has been prolonged and the quality of life has improved. However, the aggressive subtype, NSCLC, has limited treatment options.[12] Herein, it was revealed that EC-derived Evs delivered miR-376c and suppressed the proliferation, migration and invasion of NSCLC cells. In addition, miR-376c delivered by EC-derived Evs was responsible for the decreased YTHDF1 expression and the blocked Wnt/β-catenin pathway in NSCLC cells. Therefore, these findings indicated that miR-376c delivered by EC-derived may inhibit the progression of NSCLC through the YTHDF1-mediated Wnt/β-catenin pathway.

The miR-376 family is located at the distal end of mouse chromosome 12 and on chromosome 14 in humans. It comprises 3 members, miR-376a2, miR-376b and miR-376c (previously termed as miR-368).[13] miR-376c-3p has been found to be diminished in oral squamous cancer tissues and cells relative to the normal ones, and the upregulation of miR-376c-3p suppresses viability, invasion and migration, whereas it facilitates the apoptosis of SCC-25 cells.[14] These findings are in accordance with one of the major findings in the present study, which demonstrated that miR-376c restoration suppressed the viability, invasion and migration of NSCLC cells, whereas it potentiated their apoptosis. Consistently, miR-376c-3p has been shown to be poorly expressed in gastric cancer cells in
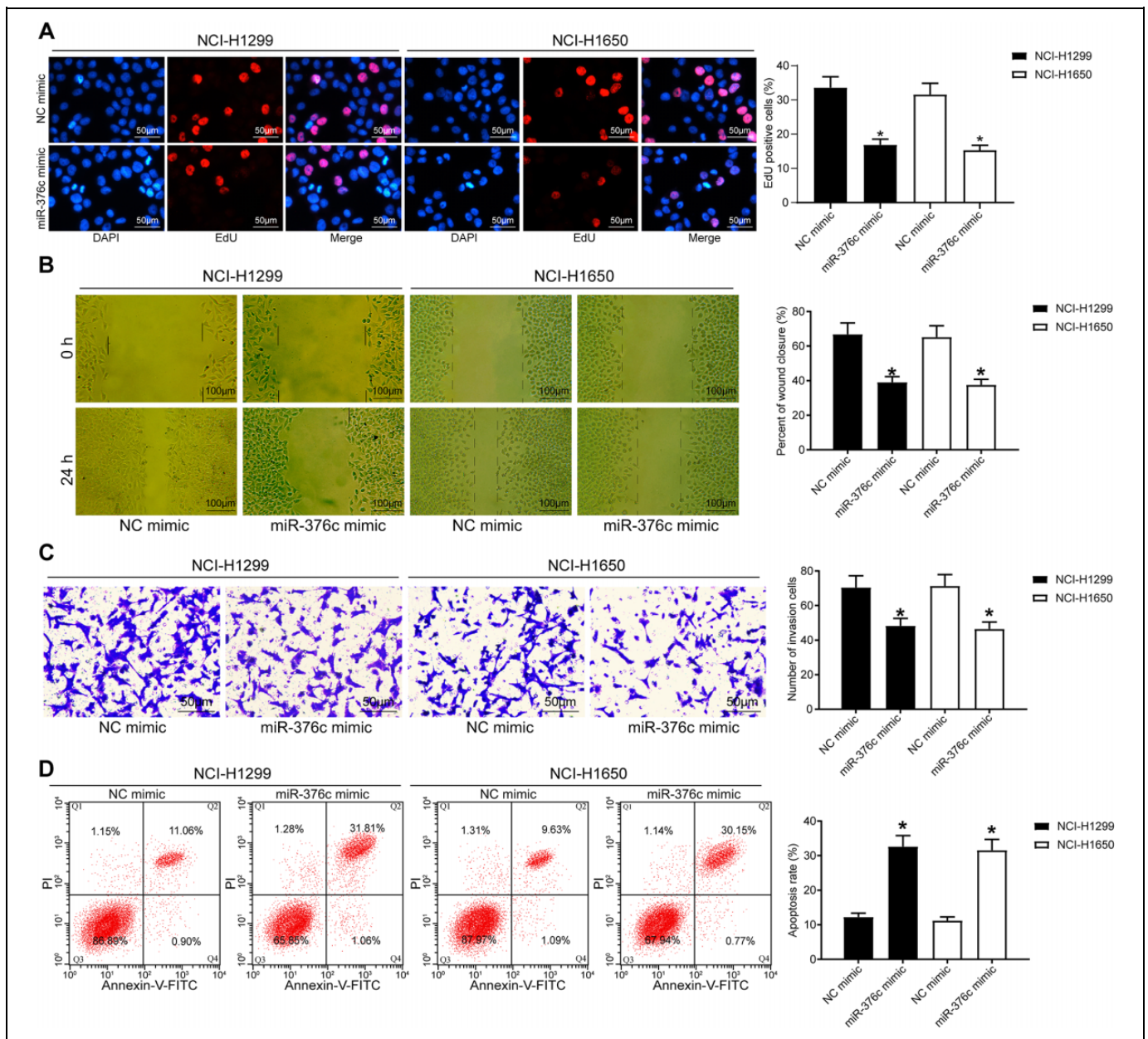
Figure 6. miR-376c released from EC-Evs impairs the proliferation, migration and invasion of NSCLC cells. (A) The cellular growth was analyzed by EdU assay in NSCLC cells (×200); (B) the cell migration capacity was analyzed by wound healing assay (×100); (C) the cell invasion capacity was analyzed by Transwell assay (×100); (D) the apoptosis rate of cells was detected by flow cytometry. *$p < 0.05$ *vs.* NSCLC cells co-cultured with ECs transfected with NC mimic. Statistical data were measurement data, and described as mean $\pm$ standard deviation. The one-way analysis of variance with Tukey's post hoc test was used for comparison among multiple groups. The experiment was repeated 3 times independently.

comparison with the normal cells, and miR-376c-3p restoration has been shown to attenuate cell proliferation and migration in gastric cancer.[15] The enforced expression of miR-376c has also been shown to inhibit cell proliferation, cell cycle and invasion of laryngeal squamous cell carcinoma cells by acting as a sponge of a lncRNA DLX6-AS1.[16] Even though the tumor inhibitory role of miR-376c has been investigated in NSCLC,[7] the detailed underlying mechanisms remain to be determined. The pro-healing function of endothelial progenitor cells-

derived exosomes has been highlighted in diabetic rats.[17] Moreover, miRNAs have been indicated to play a significant role in transmitting signals between cells via Evs under several experimental conditions.[18] Of note, the co-culture of small cell lung cancer cells with human brain microvascular ECs was shown to promote S100A16 expression, whereas GW4869, an inhibitor of exosomes, significantly disrupted this effect in the co-cultured small cell lung cancer cells.[19] Similarly, the addition of GW4869 reversed the inhibitory effects of
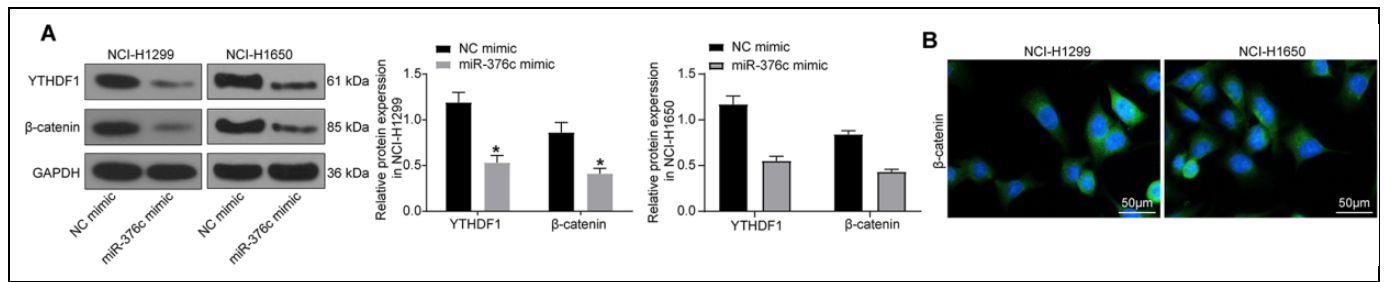
Figure 7. Release of miR-376c from EC-Evs inhibits activation of the Wnt/β-catenin pathway in NSCLC cells. (A) the protein expression of YTHDF1 and β-catenin in NSCLC cells examined by western blot analysis; (B) the location of β-catenin determined by immunofluorescence staining, where green fluorescence represents β-catenin, blue is DAPI-stained nuclei. *$p < 0.05$ *vs.* NSCLC cells co-cultured with ECs transfected with NC mimic. Statistical data were measurement data, and described as mean ± standard deviation. The one-way analysis of variance with Tukey's post hoc test was used for comparison among multiple groups. The experiment was repeated 3 times independently.
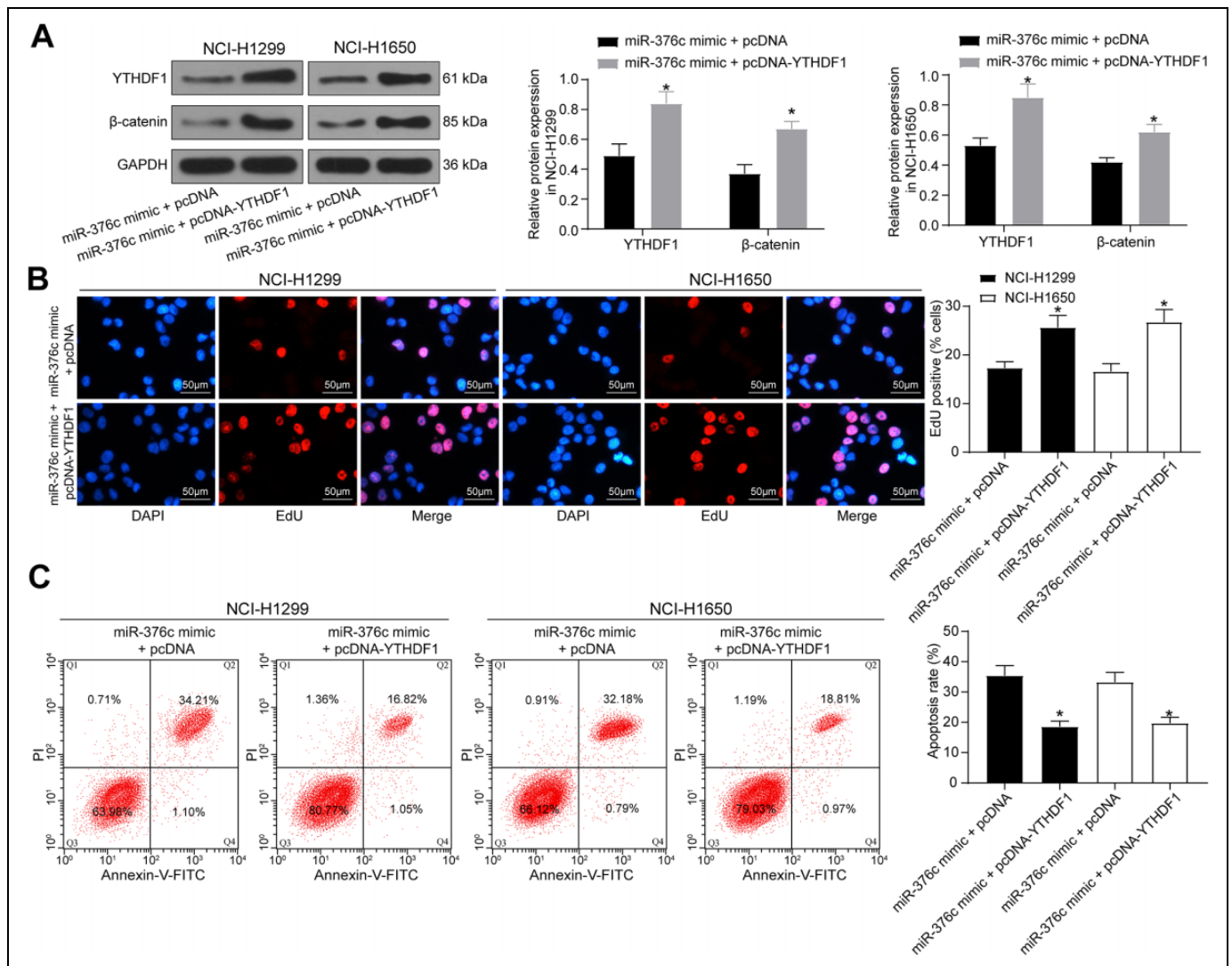

Figure 8. Overexpression of YTHDF1 attenuates the inhibitory effect of miR-376c released from EC-Evs on NSCLC cell growth. (A) The protein expression of YTHDF1 and β-catenin in NSCLC cells examined by western blot analysis; (B) the cellular growth was analyzed by EdU assay in NSCLC cells (×200); (C) the apoptosis rate of cells was detected by flow cytometry. *$p < 0.05$ *vs.* NSCLC cells co-cultured with ECs transfected with miR-376c mimic + pcDNA. Statistical data were measurement data, and described as mean ± standard deviation. The one-way analysis of variance with Tukey's post hoc test was used for comparison among multiple groups.
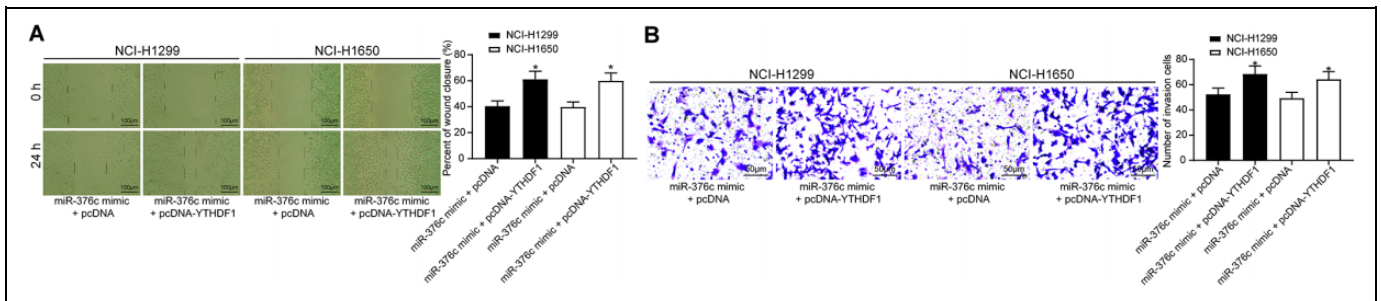
Figure 9. Overexpression of YTHDF1 attenuates the inhibitory effect of miR-376c released from EC-Evs on NSCLC cell aggressiveness. (A) The cell migration capacity was analyzed by wound healing assay (×100); (B) the cell invasion capacity was analyzed by Transwell assay (×100). *p < 0.05 *vs.* NSCLC cells co-cultured with ECs transfected with miR-376c mimic + pcDNA. Statistical data were measurement data, and described as mean $\pm$ standard deviation. The one-way analysis of variance with Tukey's post hoc test was used for comparison among multiple groups.
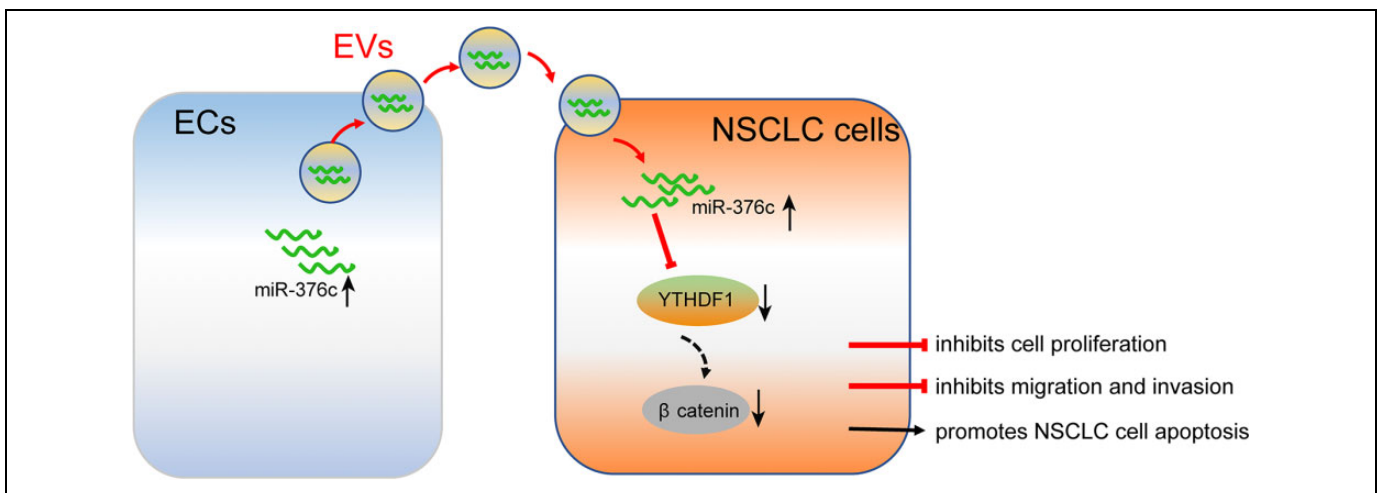

Figure 10. A schematic model for a feedback loop between EC-Evs carrying miR-376c and the NSCLC cells. EC-Evs could deliver miR-376c to NSCLC cells to downregulate YTHDF1 expression, thus repressing cell proliferation, migration and invasion, while promoting apoptosis through blocking the Wnt/β-catenin pathway.

miR-376c in NSCLC cell growth induced by miR-376c mimic in the present study, suggesting that miR-376c can be transferred from EC-Evs to NSCLC cells to play its role in the NSCLC malignant phenotype. Moreover, bioinformatics analyses and luciferase activity assays demonstrated that miR-376c could bind to YTHDF1 in the present study.

The molecular mechanisms through which YTHDF1 protein exerts its functions are principally unidentified, and it also remains uncertain as to how it is regulated due to the phase separation property.[20] YTHDF1 has been identified as an important regulator of tumor immune evasion and a probable therapeutic maneuver for improving the clinical response to immune checkpoint disruption.[21] In addition, the m6A RNA methylation regulator YTHDF1 could be applied as a prognostic factor for colon cancer, which also has possible values for the treatment of colon cancer.[22] More specifically, YTHDF1 deficiency has been substantiated to suppress NSCLC cell proliferation and the progression of de novo lung adenocarcinomas.[23] Additionally, it was hypothesized that high invasion under low m6A conditions was evoked through the Wnt-mediated E-cadherin suppression, possibly modulated by the deletion of m6A on Wnt/PI3K-Akt components in gastric cancer.[24] As we have mentioned above, miR-376c blocked the Wnt/β-catenin signaling activity in NSCLC cells. The Wnt/β-catenin signaling has been widely investigated in NSCLC, modulated by different mRNAs, miRNAs or long non-coding RNAs.[25-28] Moreover, Wnt-3 was previously verified to share a targeting association with miR-376c during osteogenesis, while miR-376c overexpression contributed to the blockage of the canonical Wnt/β-catenin pathway.[29] miR-145 has been proposed to target the 6A reader protein YTHDF2 in hepatocellular carcinoma cells.[30] Consequently, it can be hypothesized that miR-376c downregulated YTHDF1 expression to disrupt the Wnt/β-catenin pathway.

In conclusion, EC-derived Evs carrying miR-376c were demonstrated to exert negative effects on the regulation of NSCLC cell viability, migration and invasion by disrupting the Wnt/β-catenin pathway through YTHDF1 (Figure 10); these findings may provide novel therapeutic strategies for NSCLC. In addition, miRNAs are possible therapeutic targets, and

clinical trials of miRNA replacement therapy is underway.[31] Further efforts should be directed at improving the understanding of the interaction between YTHDF1 and the Wnt/β-catenin pathway as well as the potential of EC-derived Evs carrying miRNAs on NSCLC cells.

Authors' Note

All the data generated or analyzed during this study are included in this published article.

Declaration of Conflicting Interests

The author(s) declared no potential conflicts of interest with respect to the research, authorship, and/or publication of this article.

Funding

The author(s) received no financial support for the research, authorship, and/or publication of this article.

ORCID iD

Zhentian Liu 🔟 https://orcid.org/0000-0002-7733-3407

References

1. Bray F, Ferlay J, Soerjomataram I, Siegel RL, Torre LA, Jemal A. Global cancer statistics 2018: GLOBOCAN estimates of incidence and mortality worldwide for 36 cancers in 185 countries. *CA Cancer J Clin*. 2018;68(6):394-424.

2. Feng B, Zhang K, Wang R, Chen L. Non-small-cell lung cancer and miRNAs: novel biomarkers and promising tools for treatment. *Clin Sci (Lond)*. 2015;128(10):619-634.

3. Raposo G, Stoorvogel W. Extracellular vesicles: exosomes, microvesicles, and friends. *J Cell Biol*. 2013;200(4):373-383.

4. Maia J, Caja S, Strano Moraes MC, et al. Exosome-based cell-cell communication in the tumor microenvironment. *Front Cell Dev Biol*. 2018;6:18.

5. Zhang YZ, Liu F, Song CG, Couto N, Costa-Silva B. Exosomes derived from human umbilical vein endothelial cells promote neural stem cell expansion while maintain their stemness in culture. *Biochem Biophys Res Commun*. 2018;495(1): 892-898.

6. Ebrahimi A, Sadroddiny E.MicroRNAs in lung diseases: recent findings and their pathophysiological implications. *Pulm Pharmacol Ther*. 2015;34:55-63.

7. Jiang W, Tian Y, Jiang S, Liu S, Zhao X, Tian D. MicroRNA-376c suppresses non-small-cell lung cancer cell growth and invasion by targeting LRH-1-mediated Wnt signaling pathway. *Biochem Biophys Res Commun*. 2016;473(4):980-986.

8. Jia L, Zhou X, Huang X, et al. Maternal and umbilical cord serum-derived exosomes enhance endothelial cell proliferation and migration. *FASEB J*. 2018;32(8):4534-4543.

9. Zhao X, Chen Y, Mao Q, et al. Overexpression of YTHDF1 is associated with poor prognosis in patients with hepatocellular carcinoma. *Cancer Biomark*. 2018;21(4):859-868.

10. Bai Y, Yang C, Wu R, et al. YTHDF1 regulates tumorigenicity and cancer stem cell-like activity in human colorectal carcinoma. *Front Oncol*. 2019;9:332.

11. Zhang H, Bai M, Deng T, et al. Cell-derived microvesicles mediate the delivery of miR-29a/c to suppress angiogenesis in gastric carcinoma. *Cancer Lett*. 2016;375(2):331-339.

12. Jin D, Guo J, Wu Y, et al. m(6)A mRNA methylation initiated by METTL3 directly promotes YAP translation and increases YAP activity by regulating the MALAT1-miR-1914-3p-YAP axis to induce NSCLC drug resistance and metastasis. *J Hematol Oncol*. 2019;12(1):135.

13. Bhavsar SP, Lokke C, Flaegstad T, Einvik C. Hsa-miR-376c-3p targets Cyclin D1 and induces G1-cell cycle arrest in neuroblastoma cells. *Oncol Lett*. 2018;16(5):6786-6794.

14. Wang K, Jin J, Ma T, et al. MiR-376c-3p regulates the proliferation, invasion, migration, cell cycle and apoptosis of human oral squamous cancer cells by suppressing HOXB7. *Biomed Pharmacother*. 2017;91:517-525.

15. Liu B, Li G, Zhang Z, Wu H. Influence of miR-376c-3p/SYF2 axis on the progression of gastric cancer. *Technol Cancer Res Treat*. 2019;18:1533033819874808.

16. Yang Q, Sun J, Ma Y, Zhao C, Song J. LncRNA DLX6-AS1 promotes laryngeal squamous cell carcinoma growth and invasion through regulating miR-376c. *Am J Transl Res*. 2019;11(11): 7009-7017.

17. Li X, Jiang C, Zhao J. Human endothelial progenitor cells-derived exosomes accelerate cutaneous wound healing in diabetic rats by promoting endothelial function. *J Diabetes Complications*. 2016; 30(6):986-992.

18. Yue KY, Zhang PR, Zheng MH, et al. Neurons can upregulate Cav-1 to increase intake of endothelial cells-derived extracellular vesicles that attenuate apoptosis via miR-1290. *Cell Death Dis*. 2019;10(12):869.

19. Xu ZH, Miao ZW, Jiang QZ, et al. Brain microvascular endothelial cell exosome-mediated S100A16 up-regulation confers small-cell lung cancer cell survival in brain. *FASEB J*. 2019;33(2): 1742-1757.

20. Gao Y, Pei G, Li D, et al. Multivalent m(6)A motifs promote phase separation of YTHDF proteins. *Cell Res*. 2019;29(9): 767-769.

21. The m(6)A-Binding Protein YTHDF1 mediates immune evasion. *Cancer Discov*. 2019;9(4):461.

22. Liu T, Li C, Jin L, Li C, Wang L. The prognostic value of m6A RNA methylation regulators in colon adenocarcinoma. *Med Sci Monit*. 2019;25:9435-9445.

23. Shi Y, Fan S, Wu M, et al. YTHDF1 links hypoxia adaptation and non-small cell lung cancer progression. *Nat Commun*. 2019;10(1): 4892.

24. Zhang C, Zhang M, Ge S, et al. Reduced m6A modification predicts malignant phenotypes and augmented Wnt/PI3K-Akt signaling in gastric cancer. *Cancer Med*. 2019;8(10): 4766-4781.

25. Gu B, Wang J, Song Y, Wang Q, Wu Q. microRNA-383 regulates cell viability and apoptosis by mediating Wnt/beta-catenin signaling pathway in non-small cell lung cancer. *J Cell Biochem*. 2018.

26. Liu T, Wu X, Chen T, Luo Z, Hu X. Downregulation of DNMT3A by miR-708-5p inhibits lung cancer stem cell-like phenotypes through repressing Wnt/beta-catenin signaling. *Clin Cancer Res*. 2018;24(7):1748-1760.

27. Wang T, Liu X, Tian Q, Liang T, Chang P. Reduced SPOCK1 expression inhibits non-small cell lung cancer cell proliferation and migration through Wnt/beta-catenin signaling. *Eur Rev Med Pharmacol Sci*. 2018;22(3):637-644.

28. Zhao C, Qiao C, Zong L, Chen Y. Long non-coding RNA-CCAT2 promotes the occurrence of non-small cell lung cancer by regulating the Wnt/beta-catenin signaling pathway. *Oncol Lett*. 2018; 16(4):4600-4606.

29. Kureel J, John AA, Prakash R, Singh D. MiR 376c inhibits osteoblastogenesis by targeting Wnt3 and ARF-GEF-1—facilitated augmentation of beta-catenin transactivation. *J Cell Biochem*. 2018;119(4):3293-3303.

30. Yang Z, Li J, Feng G, et al. MicroRNA-145 modulates N(6)-methyladenosine levels by targeting the 3'-untranslated mRNA region of the N(6)-methyladenosine binding YTH domain family 2 protein. *J Biol Chem*. 2017;292(9): 3614-3623.

31. Yoshida K, Yokoi A, Kato T, Ochiya T, Yamamoto Y. The clinical impact of intra- and extracellular miRNAs in ovarian cancer. *Cancer Sci*. 2020;111(10):3435-3444.